Time Domain Reshuffling for OFDM based Indoor Visible Light Communications

Xiaodi You[1], Jian Chen[1,*], Changyuan Yu[2], Zabih Ghassemlooy[3]
[1]School of Telecommunications & Information Engineering, Nanjing University of Posts & Telecommunications, Nanjing, China
[2]Department of Electronic & Information Engineering, The Hong Kong Polytechnic University, Hong Kong
[3]Faculty of Engineering & Environment, University of Northumbria at Newcastle, Newcastle Upon Tyne, UK
*Email: chenjian@njupt.edu.cn

***Abstract*—For orthogonal frequency division multiplexing (OFDM) based indoor visible light communication (VLC) systems, we show that the subcarrier channels tend to synchronize and add up to a resultant high peak signal at the leading edge of each symbol when using certain types of modulation formats. Thus, occasional non-ideal transmission conditions such as insufficient guard intervals and a dispersive channel will result in inter-symbol crosstalk. This paper presents a time domain reshuffling (TDR) technique for both DC-biased optical (DCO-) and asymmetrically clipped optical (ACO-) OFDM based VLC systems. Only by simple operations in the frequency domain, the potential high peaks can be relocated in each OFDM symbol to alleviate the crosstalk. Based on Monte-Carlo simulations, we demonstrate the statistical distribution of the signal high peak values and the complementary cumulative distribution function of the peak-to-average power ratio for comparison. By adopting the TDR method, we show that the bit error rate performance can be also improved for both DCO- and ACO-OFDM systems under occasional non-ideal transmission conditions.**

Keywords—Visible light communications; DCO-OFDM; ACO-OFDM; time domain reshuffling.

I. INTRODUCTION

Recently, visible light communication (VLC) has become an intriguing alternative to the radio frequency wireless technologies due to its advantages including unregulated huge bandwidth, high energy efficiency, multiple functionalities, green technology, etc. [1]. Orthogonal frequency division multiplexing (OFDM), with successful implementation in both optical fiber and radio frequency based systems, has been introduced to indoor VLC systems owing to its robustness against the multi-path induced dispersion due to light reflections [2]−[4]. Since current commercial optical components do not allow the phase as the mean to convey data information, then the coherent OFDM frames cannot be translated directly into incoherent VLC systems. The intensity modulation with direct detection (IM/DD) scheme is the most widely adopted option in VLC due to its simplicity and robustness [5]. There are generally two popular types of IM/DD OFDM schemes in VLC systems: DC-biased optical OFDM (DCO-OFDM) and asymmetrically clipped optical OFDM (ACO-OFDM) [6].

In high-speed indoor VLC applications, an OFDM frame is very likely to interfere with its neighboring symbols when the link experiences random multi-path delay, obstruction, user's mobility, loss of synchronization, etc. [7]. OFDM systems are inherently designed to have sufficient guard interval (GI), which could be as long as the channel's impulse response to allow for frequency domain equalization and power/bit loading. Although adopting GI can reduce the inter-symbol interference and inter-carrier interference, the system data throughput can be reduced if GI length is too long. Schemes with shorter GI and with no GI have been reported in optical fiber systems [8], [9]. In [8] reduced GI overhead was achieved by means of digital sub-band demultiplexing, whereas in [9], the coherent OFDM scheme with no GI for 100 Gb/s long-haul transmission was realized using equalization and filtering techniques at the receiver (Rx). For VLC systems with insufficient GI, part of the signal, especially at the marginal position of an OFDM frame, will still interfere with its neighboring symbols under some conditions. This is best illustrated in Fig. 1 for the scenario with no GI, where the leading edge of the next symbol (shadowed region) overlaps with the current OFDM symbol, i.e., the current fast Fourier transform (FFT) window, at the Rx. This overlap consequently leads to the inter-symbol crosstalk (ISC), which needs to be reduced in order to maintain the required link performance.

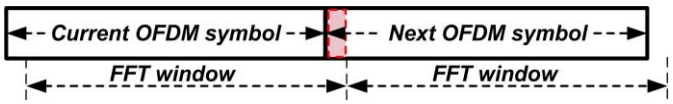

Fig. 1. Schematic diagram of the crosstalk between OFDM symbols w/o GI.

The concept of parallel transmission to equivalently extend the symbol length is the key in OFDM systems. As a result, the high peak-to-average power ratio (PAPR) in VLC systems is a major issue, which has been extensively investigated in the literatures [10]−[14]. In [12] the PAPR was effectively reduced by using the discrete Fourier transform (DFT) spread technique, whereas in [13] and [14], IM/DD OFDM structures with lower PAPR were proposed. In this paper the aim is not to investigate PAPR reduction techniques. Instead, we focus on the distribution characteristic of the signal peak values in the time domain of OFDM symbols. Based on the conventional DCO- and ACO-OFDM systems, we first demonstrate that for certain types of modulation formats, transmitting signals using a number of parallel subcarrier channels can have higher probability of being combined with a

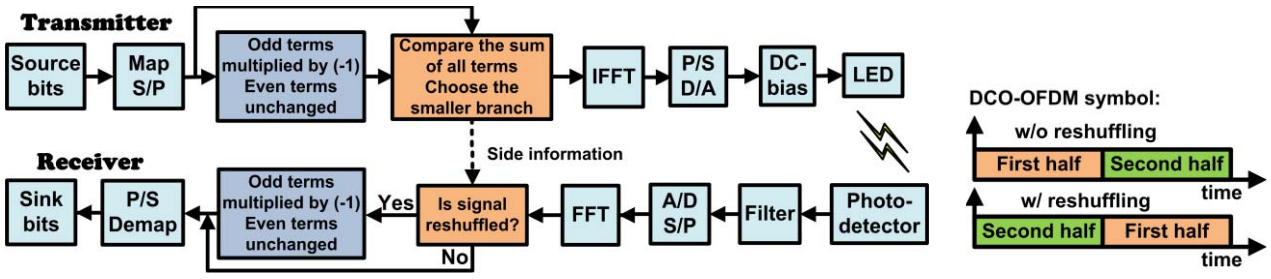

(a) (b)

Fig. 2. (a) Block diagram of the TDR method for DCO-OFDM systems; and (b) Schematic diagram of the TDR method for a DCO-OFDM symbol.

resultant high peak at the leading edge of each OFDM symbol. This means that the leading edge of an OFDM symbol is more likely to contain a considerable proportion of the signal energy and thus should be properly taken care of. Otherwise it will severely affect the demodulation performance. To solve this problem, we propose a time domain reshuffling (TDR) method for both DCO- and ACO-OFDM systems. Through simple preprocessing procedures in the frequency domain, the potential high peaks can be relocated within each OFDM symbol without the need for buffering and exchanging long data block sequences in the time domain, thus effectively alleviating the ISC. Based on Monte-Carlo simulations, the distribution of the high peaks within OFDM symbols and the complementary cumulative distribution function (CCDF) of the PAPR are demonstrated for comparison. We show that the system bit error rate (BER) performance can be also improved by adopting the TDR method for non-line of sight transmission conditions.

The rest of the paper is outlined as follow. The principle of the proposed TDR scheme for DCO- and ACO-OFDM will be presented in Sections 2 and 3, respectively. Numerical simulation results are shown in Section 4 and finally we provide a summary in Section 5.

II. TDR FOR DCO-OFDM SYSTEMS

A. Principle

In conventional OFDM systems, the data information is encoded in the frequency domain and are transmitted in a number of parallel orthogonal subcarriers. This is generally implemented using an inverse FFT (IFFT). The generated discrete OFDM signal in the time domain is given as [4]:

$$s(n) = (\sqrt{1/N_c}) \sum_{k=0}^{N_c-1} S(k) e^{j2\pi nk/N_c}, n = 0,1,\cdots N_c - 1, \quad (1)$$

where $S(k)$ is the complex symbol mapped on the kth subcarrier channel, and N_c is the total channel number. For DCO-OFDM, the input signal of IFFT should satisfy the Hermitian symmetry property to produce real values. Following IFFT, a DC bias is added to the bipolar real values to generate the strictly positive signal. Considering the total channel number N_c to be $2N$ for DCO-OFDM, the Hermitian symmetry is defined as [6]:

$$\{S(k)\}_{k=0}^{2N-1} = [0 \ \ \{X_k\}_{k=1}^{N-1} \ \ 0 \ \ \{X_k^*\}_{k=N-1}^{1}], \quad (2)$$

where X_k is the complex symbol to be transmitted. Thus, the discrete time domain signal of DCO-OFDM is expressed by:

$$s(n) = (\sqrt{2/N}) \sum_{k=1}^{N-1} [a_k \cos(\pi nk/N) - b_k \sin(\pi nk/N)], n = 0,1,\cdots 2N-1, \quad (3)$$

where a_k and b_k are the real and imaginary parts of X_k, respectively. For each sampling point $s(n)$ in the time domain, while the average value is always zero, the variance can be given by:

$$Var[s(n)] = (1/N) \sum_{k=1}^{N-1} \{[Var(a_k) - Var(b_k)] \cos(2\pi nk/N) + Var(a_k) + Var(b_k)\}. \quad (4)$$

If $Var(a_k)$ and $Var(b_k)$ are the same, then the variance of $s(n)$ is considered to be constant. However, for certain types of modulation formats, including binary phase shift keying (BPSK), rectangle 8-quadrature amplitude modulation (QAM) and so on [15]–[18], $Var(a_k) > Var(b_k)$. Take a rectangle 8-QAM as an example, with the constellation points in the first quadrant of (1, 1) and (3, 1), $Var(a_k)$ and $Var(b_k)$ are then $(3^2+1^2)/2$ and 1^2, respectively. Thus, according to (4), when the index n is zero, the variance of $s(n)$ will be larger than the average power of OFDM signal. Actually, the amplitude of the sampling point $s(0)$ in the time domain is proportional to the cumulative sum of a_k. Therefore, $s(0)$ has a higher chance to form a resultant high peak than other positions. Note that the peak signal discussed in this paper is the absolute value, which includes both positive and negative peak values. However, in dispersive channels, the OFDM symbol leading edge will be outside the FFT window at the Rx, see Fig. 1. Consequently, the link will experience severe ISC if $s(0)$ happens to be a high peak.

In order to solve this problem, we propose a new scheme of TDR method for DCO-OFDM systems as illustrated in Fig. 2(a). The operation is the same as the conventional DCO-OFDM scheme, except for the preprocessing procedures prior to IFFT at the transmitter (Tx), which is being made simple by only changing the sign of odd subcarrier channels while keeping the even subcarrier channels unchanged. For the proposed scheme, the generated discrete OFDM signal is expressed as:

$$f(n) = (\sqrt{1/2N}) \sum_{k=0}^{2N-1} (-1)^k S(k) e^{j\pi nk/N}, n = 0,1,\cdots 2N-1. \quad (5)$$

Reverse procedures are adopted to recover the original data at the Rx. The $(-1)^k$ sequence in (5) can be seen as the discrete sampling points of a periodic trigonometric function. Therefore, multiplying this sequence in the frequency domain represents a convolution between the OFDM signal and the impulse function at a specific time delay in the time domain [19]. As a result, each OFDM symbol is equivalently

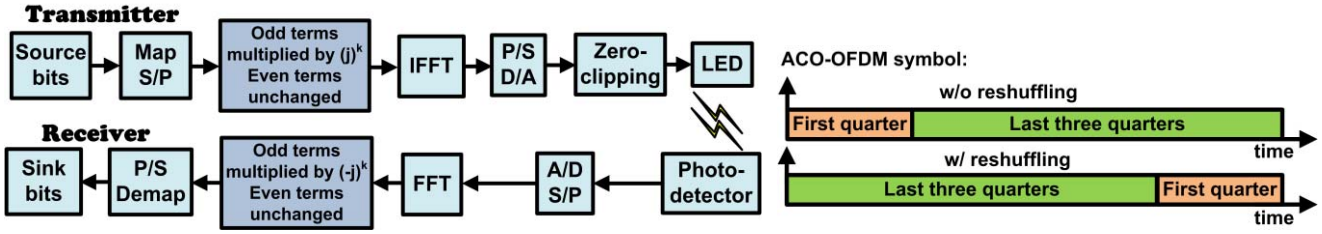

(a) (b)

Fig. 3. (a) Block diagram of the TDR method for ACO-OFDM systems; and (b) Schematic diagram of the TDR method for an ACO-OFDM symbol.

exchanging its first half with the second half, thus the *time domain reshuffling* concept, which is represented by:

$$f(n) = s(n+N) \text{ if } 0 \le n < N \text{ or } s(n-N) \text{ if } N \le n < 2N. \quad (6)$$

Fig. 2(b) also shows the schematic diagram of the TDR method for a DCO-OFDM symbol. In general, in order to reshuffle the OFDM signal, we may need complex procedures such as buffering and exchanging the long data block sequence in the time domain. However, by adopting parallel preprocessing for the subcarrier channels in the frequency domain, we can simply reshuffle the OFDM signal without the need for buffering and exchanging procedures, which saves both storage and time.

B. Comparison module

From (6), the potential high peaks at the symbol leading edge can be moved to the middle part of the symbol by means of reshuffling. To be more specific, the targeted sampling point $s(0)$ in the time domain is exchanged with $s(N)$. However, it is not difficult to show that $s(N)$ is actually proportional to the cumulative sum of $(-1)^k a_k$. This means that the subcarrier channels still tend to add up to a high peak at $s(N)$. In this case, the link will still experience ISC if only the simple reshuffling scheme is used. For instance, if $s(N)$ carries more energy than $s(0)$ in the original OFDM frame, then only using simple reshuffling will worsen the link performance. Thus, we propose to include a comparison module, as shown in the orange blocks of Fig. 2(a). By comparing $s(0)$ with $s(N)$, reshuffling will be conducted selectively to ensure that the actual higher peak is within each symbol. Specifically, reshuffling is conducted only when

$$\left|\sum_{k=0}^{2N-1} S(k)\right| > \left|\sum_{k=0}^{2N-1} (-1)^k S(k)\right|. \quad (7)$$

From (7), the computation of this module only involves the sum of subcarrier channels, which is totally linear and parallel to maintain the high efficiency and the low latency features. Note that only 1 bit of side information [20]−[22] per OFDM frame is transmitted to inform the Rx if the signal is being reshuffled. Compared with retransmitting the distorted peak value at the leading edge, transmitting a single bit each time for performance improvement is a worthwhile strategy. The reserved symmetric channels can be also used to record the occurrence of reshuffling. However, this exerts almost no effect on the previous outcomes of the comparison procedure.

III. TDR FOR ACO-OFDM SYSTEMS

In conventional ACO-OFDM systems, the data information is only mapped to the odd IFFT inputs. Compared with DCO-OFDM, all even inputs are set to zero. Considering the total channel number N_c to be $4N$ for ACO-OFDM, the arrangement of complex symbols on the subcarrier channels should be as [6]:

$$\{S_k\}_{k=0}^{4N-1} = [0 X_1 0 X_2 ... 0 X_N 0 X_N^* 0 ... X_2^* 0 X_1^*]. \quad (8)$$

Based on the analysis in Section 2, the time domain signal of ACO-OFDM still tends to have a resultant high peak at the symbol leading edge similar to DCO-OFDM. However, the reshuffling method adopted for DCO-OFDM is not applicable in ACO-OFDM systems due to the different allocation of complex symbols. Here we propose a TDR method for ACO-OFDM as shown in Fig. 3(a). The procedure is similar to the TDR method of DCO-OFDM, where the even subcarrier channels are kept unchanged and the odd subcarrier channels are multiplied by the $(j)^k$ sequence. This sequence can be also regarded as the discrete sampling points of a periodic trigonometric function. The generated discrete OFDM signal is then given as:

$$f(n) = (\sqrt{1/4N}) \sum_{k=0}^{4N-1} (j)^k S(k) e^{j\pi nk/(2N)}, n = 0,1,\cdots 4N-1. \quad (9)$$

As a result, each OFDM symbol is equivalently exchanging its first quarter with the rest of the symbol. The potential high peaks at the symbol leading edge are then moved to within the symbol. This process can be described as:

$$f(n) = s(n+3N) \text{ if } 0 \le n < N \text{ or } s(n-N) \text{ if } N \le n < 4N. \quad (10)$$

Note that for TDR of ACO-OFDM symbols, we can also multiply the odd subcarrier channels by the $(-j)^k$ sequence instead of the $(j)^k$ sequence in (9) while keeping the even subcarrier channels unchanged. As a result, each OFDM symbol is equivalently exchanging its last quarter with the rest of the symbol. Without loss of generality, this paper will only consider the case of adopting the $(j)^k$ sequence for ACO-OFDM. The schematic diagram of the TDR method for an ACO-OFDM symbol is also demonstrated in Fig. 3(b). By adopting reshuffling, the targeted $s(0)$ is exchanged with $s(N)$. In Section 4, we will show that high peaks are less likely to appear at $s(N)$ compared with $s(0)$ in ACO-OFDM systems. Although using a comparison module will improve the system performance to a certain degree, we do not include it in the ACO-OFDM system for consideration of the system work load and the spectral efficiency.

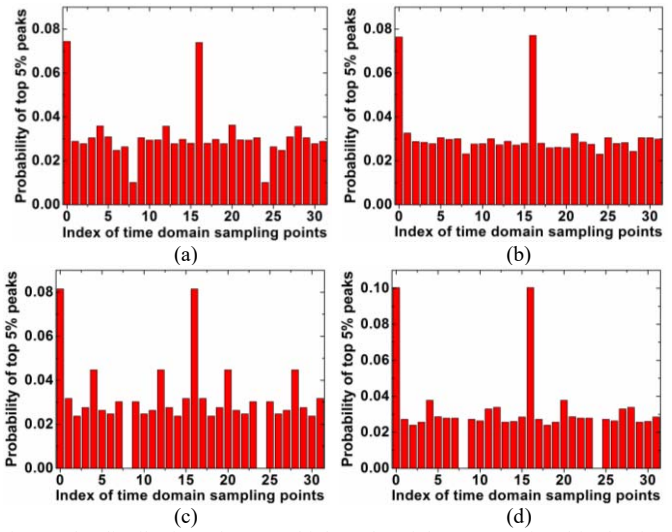

Fig. 4. The distribution of top 5% high peaks of the OFDM signal in the time domain w/o reshuffling: (a) DCO-OFDM with BPSK; (b) DCO-OFDM with rectangle 8-QAM; (c) ACO-OFDM with BPSK; and (d) ACO-OFDM with rectangle 8-QAM. Here a total of 32 subcarrier channels are considered.

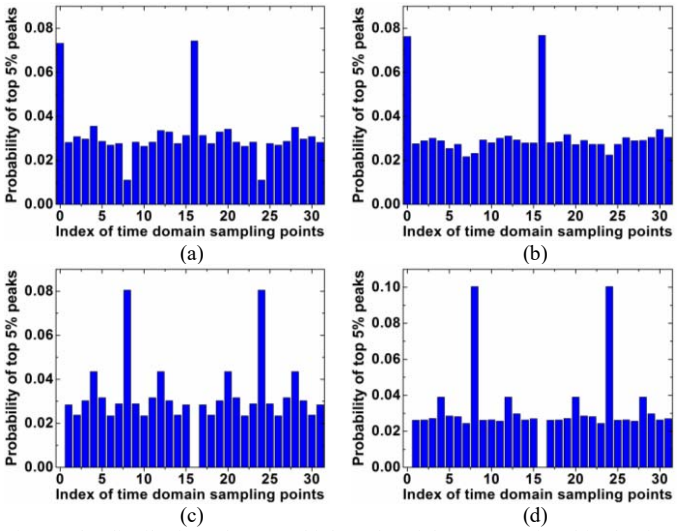

Fig. 5. The distribution of top 5% high peaks of the OFDM signal in the time domain w/ reshuffling: (a) DCO-OFDM with BPSK; (b) DCO-OFDM with rectangle 8-QAM; (c) ACO-OFDM with BPSK; and (d) ACO-OFDM with rectangle 8-QAM. Here a total of 32 subcarrier channels are considered.

IV. Simulation and Discussions

In this section, a pseudo-random sequence, adopted as the source stream, is to be modulated on parallel subcarrier channels. For each figure, more than 10^4 of OFDM frames are tested in Monte-Carlo simulations. Modulation formats with variance of the real part a_k being larger than the imaginary part b_k will be considered. For modulation formats such as quadrature phase shift keying (QPSK), $Var(a_k) = Var(b_k)$, thus the reshuffling method will not lead to performance improvement according to the discussion in Section 2. However, as long as $Var(a_k) > Var(b_k)$, reshuffling will be an effective solution to overcome the ISC. For instance, in OFDM based VLC systems, the bit loading scheme has been adopted as in [23]. When transmitting BPSK and QPSK signals in different subcarrier channels at the same time, $Var(a_k)$ will be larger than $Var(b_k)$. Thus, the reshuffling

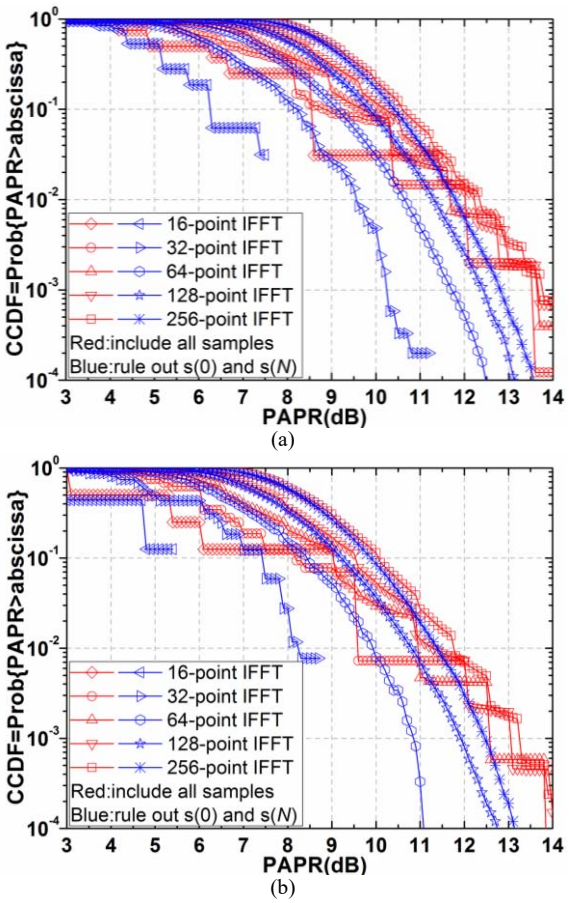

Fig. 6. The CCDFs of the PAPR for: (a) DCO-OFDM and (b) ACO-OFDM. Here BPSK is considered as an example.

method is still applicable to such hybrid systems. In this section, we focus on BPSK and rectangle 8-QAM, which represent the cases of zero and non-zero value of b_k, respectively. Other higher modulation formats such as rectangle 32-QAM and other hybrid modulation schemes will be analyzed in the future work.

In Figs. 4 and 5, the distributions of top 5% high peaks for DCO- and ACO-OFDM time domain signals with and without reshuffling are illustrated, respectively. Note that if top 1% and 10% high peaks or larger subcarrier numbers are considered, a similar distribution can be observed. Here we only show the representative 5% case with a total of 32 subcarrier channels. From Figs. 4(a) and (b), subcarrier channels of the conventional DCO-OFDM signal exactly synchronize at the positions of the discrete time domain signal $s(0)$ and $s(16)$. High peaks have more probability to occur here than any other positions. Thus, with reshuffling, DCO-OFDM symbols still tend to have high peaks at the leading side. Observe that Figs. 5(a) and (b) display similar distributions as Figs. 4(a) and (b), respectively. This means if $s(16)$ has higher energy level than $s(0)$ in the original OFDM frame, then only using simple reshuffling will not improve the link performance. Therefore, a comparison module is necessary to ensure lower energy at the OFDM symbol leading side in order to reduce the ISC. In Figs. 4(c) and (d), conventional ACO-OFDM signals are also more likely to experience high peaks at $s(0)$. Therefore, with reshuffling, $s(0)$ is relocated and

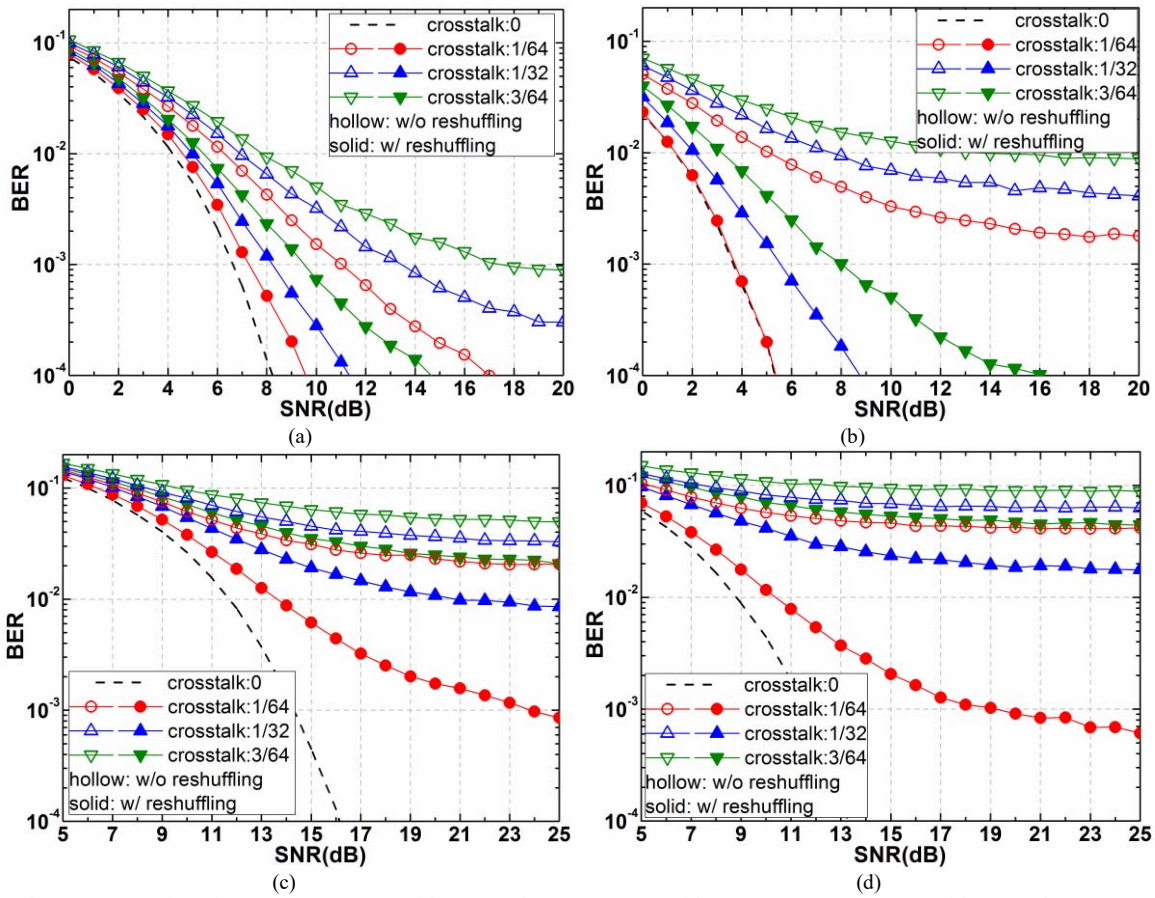

Fig. 7. BER performace comparison for: (a) DCO-OFDM with BPSK; (b) ACO-OFDM with BPSK; (c) DCO-OFDM with rectangle 8-QAM; and (d) ACO-OFDM with rectangle 8-QAM. Here a total of 64 subcarrier channels are considered.

exchanged with $s(8)$. From (1) and (8), it can readily be shown that $s(8)$ is proportional to the sum of b_k. Thus, $s(8)$ is always zero for BPSK. For rectangle 8-QAM, although b_k is non-zero, $s(8)$ still has a small probability to add up to high peaks. This is due to the much lower energy of b_k compared with a_k. Therefore, the TDR of ACO-OFDM can effectively avoid high peaks and alleviate the ISC with the low-energy $s(8)$ at the start, see Figs. 5(c) and (d). Furthermore, the comparison module adopted in DCO-OFDM is not needed in ACO-OFDM systems, thus simplifying the system design.

Fig. 6 demonstrates the simulated results of the CCDFs of the PAPR against the PAPR for DCO- and ACO-OFDM systems, respectively for a range of IFFT. The commonly used definition of CCFD can be found in [24]. In this paper, BPSK is taken as an example. Similar results can be also observed for rectangle 8-QAM. The plots in red represent the CCDFs including all time domain samples, which is discrete especially for small number of subcarriers. The discrete high PAPR is due to only a few discrete high peak values of OFDM signals. For larger subcarrier numbers, there are an increasing number of discrete peak values, which contribute to the continuous profiles of the plots. In order to explain the reason for these high peak values, we also show the plots in blue to represent the CCDFs that exclude $s(0)$ and $s(N)$ of DCO-OFDM and $s(0)$ and $s(2N)$ of ACO-OFDM, respectively. By comparison, the CCDF plots without these sampling points are much smoother and closer to the vertical axis. This means that the PAPR is exclusively reduced. Therefore, the potential high peaks at $s(0)$ and $s(N)$ of DCO-OFDM and $s(0)$ and $s(2N)$ of ACO-OFDM actually make a significant contribution to the high PAPR in conventional OFDM based VLC systems. Therefore, the TDR method can be used to effectively rearrange the positions of potential high peaks in order to alleviate the ISC.

Finally, Fig. 7 depicts the BER against the signal to noise ratio (SNR) for DCO- and ACO-OFDM systems with and without TDR, respectively, for a total of 64 subcarrier channels. Monte-Carlo simulation results with at least 100 error bits are adopted to decrease the random fluctuation. For the fundamental analysis, we have assumed the scenarios with no GI as shown in Fig. 1, and the ISC accounting for 1/64, 2/32 and 3/64 of the OFDM symbol length in a back-to-back VLC system with the additive white Gaussian noise at the Rx. For DCO-OFDM with BPSK, when the ISC is 3/64 of the OFDM symbol length, utilizing the TDR method can result in an ~8 dB of SNR gain at a BER of 10^{-3}. For ACO-OFDM with BPSK, we can observe asymptotic BER performance caused by the ISC, thus making it challenging to achieve the forward error correction (FEC) BER limit of 10^{-3} [25]. By adopting TDR for ACO-OFDM, the system BER performance can be effectively improved. At a BER of 10^{-3}, the SNR loss is less than 4.4 dB when the ISC is 3/64. The improvement is more significant for ACO-OFDM because of doubling of ISC during demodulation due to the symmetry property of the

ACO-OFDM waveform. When using rectangle 8-QAM, both DCO- and ACO-OFDM systems without TDR cannot support a reliable communication. However, by adopting the TDR method, we observe asymptotic BER plots when the ISC accounts for more than 1/32 of the OFDM symbol length. When the ISC is less than 1/64, a BER of 10^{-3} can be eventually achieved with TDR for both DCO- and ACO-OFDM systems.

V. CONCULSION

In indoor VLC systems based on OFDM, we first showed that for certain types of modulation formats with variance of the real part being larger than the imaginary part, the subcarrier channels tend to show resultant high peaks at the leading edge of each OFDM symbol. This makes the systems more vulnerable to the ISC under non-ideal transmission conditions. In order to relocate the potential peaks at the OFDM symbol leading edge, we proposed a TDR method for both DCO- and ACO-OFDM systems. The method is attractive because it can reshuffle the OFDM time domain signal by using low-complexity operations in the frequency domain. Monte-Carlo simulation results showed an improvement in the BER performance for the VLC link with a dispersive channel condition. With BPSK, at a BER of 10^{-3} and with the ISC of 3/64, the SNR gain was around 8 dB for DCO-OFDM while the SNR penalty was less than 4.4 dB for ACO-OFDM. We also demonstrated a reliable transmission by adopting TDR using rectangle 8-QAM with the ISC being less than 1/64.

References

[1] T. Komine, *et al.*, "Fundamental analysis for visible-light communication system using LED lights", *IEEE Trans. Consum. Electron.*, vol. 50, no. 1, pp. 100−107, 2004.

[2] M. Z. Afgani, *et al.*, "Visible light communication using OFDM", in *Proc. 2nd IEEE Int. Conf. TRIDENTCOM*, pp. 129–134, 2006.

[3] H. Elgala, *et al.*, "Indoor broadcasting via white LEDs and OFDM", *IEEE Trans. Consum. Electron.*, vol. 55, no. 3, pp. 1127−1134, 2009.

[4] J. Armstrong, "OFDM for optical communications", *J. Lightw. Technol.*, vol. 27, no. 3, pp. 189−204, 2009.

[5] J. Armstrong, *et al.*, "Comparison of asymmetrically clipped optical OFDM and DC-biased optical OFDM in AWGN", *IEEE Commun. Lett.*, vol. 12, no. 5, pp. 343−345, 2008.

[6] R. Mesleh, *et al.*, "On the performance of different OFDM based optical wireless communication systems", *J. Opt. Commun. Netw.*, vol. 3, no. 8, pp. 620−628, 2011.

[7] Z. Ghassemlooy, *et al.*, "*Optical wireless communications: system and channel modelling with Matlab*", Boca Raton, USA, CRC Press, 2012.

[8] B. Zhu, *et al.*, "Ultra-long-haul transmission of 1.2-Tb/s multicarrier no-guard-interval CO-OFDM superchannel using ultra-large-area fiber", *IEEE Photon. Technol. Lett.*, vol. 21, no. 11, pp. 826−828, 2010.

[9] A. Sano, *et al.*, "No-guard-interval coherent optical OFDM for 100-Gb/s long-haul WDM transmission", *J. Lightw. Technol.*, vol. 27, no. 16, pp. 3705−3713, 2009.

[10] H. Zhang, *et al.*, "PAPR reduction for DCO-OFDM visible light communications via semidefinite relaxation", *IEEE Photon. Technol. Lett.*, vol. 26, no. 17, pp. 1718−1721, 2014.

[11] W. Popoola, *et al.*, "Optimising OFDM based visible light communication for high throughput and reduced PAPR", in *Proc. IEEE Int. Conf. Comm. Workshop (ICCW)*, 1322−1326, Jun. 2015.

[12] C. Wu, *et al.*, "On visible light communication using LED array with DFT-spread OFDM", in *Proc. IEEE Int. Conf. Comm. (ICC)*, 3325−3330, Jun. 2014.

[13] D. Tsonev, *et al.*, "Novel unipolar orthogonal frequency division multiplexing (U-OFDM) for optical wireless", in *Proc. IEEE Int. Conf. VTC Spring*, 1−5, May. 2012.

[14] H. Elgala, *et al.*, "P-OFDM: spectrally efficient unipolar OFDM", in *Proc. Conf. OFC/NFOEC*, pp. Th3G. 7, Mar. 2014.

[15] A. Le, *et al.*, "A group of modulation schemes for adaptive modulation", in *Proc.IEEE Int. Conf. Comm. Systems (ICCS)*, 864−869. Nov. 2008.

[16] K. Cho, *et al.*, "On the general BER expression of one- and two-dimensional amplitude modulations", *IEEE Trans. Commun.*, vol. 50, no. 7, pp. 1074−1080, 2002.

[17] J. Luna-Rivera, *et al.*, "Constellation design for spatial modulation", *Procedia Technology*, vol. 7, no. 4, pp. 71−78, 2013.

[18] F. Kayhan, *et al.*, "Constellation design for channels affected by phase noise", in *Proc. IEEE Int. Conf. Comm.(ICC)*, 3154−3158, Jun. 2013.

[19] R. Lyons, "*Understanding Digital Signal Processing*", Prentice Hall International, 2004.

[20] A. D. Wyner, *et al.*, "The rate-distortion function for source coding with side information at the decoder", *IEEE Trans. Inf. Theory*, vol. 22, no. 1, pp. 1−10, 1976.

[21] R. W. Baum, *et al.*, "Reducing the peak-to-average power ratio of multicarrier modulation by selected mapping", *Electron. Lett.*, vol. 32, no. 22, pp. 2056−2057, 1996.

[22] L. J. Cimini, *et al.*, "Peak-to-average power ratio reduction of an OFDM signal using partial transmit sequences", *IEEE Commun. Lett.*, vol. 4, no. 3, pp. 86−88, 2000.

[23] Z. Yu, *et al.*, "PAPR reduction for bit-loaded OFDM in visible light communications", in *Proc. IEEE Int. Conf. WCNC*, 334−339, 2015.

[24] S. Han, *et al.*, "An overview of peak-to-average power ratio reduction techniques for multicarrier transmission", *Wireless Commun.*, vol. 12, no. 2, pp. 1536−1284, 2005.

[25] R. Essiambre, *et al.*, "Capacity limits of optical fiber networks", *J. Lightw. Technol.*, vol. 28, no. 4, pp. 662−701, 2010.